

SIMULATIONS OF XFEL FOR THE KEK ERL

R. Hajima[#], N. Nishimori, JAEA, Tokai, Ibaraki, 319-1195, Japan
 N. Sei, AIST, Tsukuba, Ibaraki, 305-8568, Japan
 M. Shimada, N. Nakamura, KEK, Tsukuba, Ibaraki, 305-0801, Japan

Abstract

Following the recent development of high-brightness electron guns and high-reflectivity X-ray crystal optics, an FEL oscillator operated in a hard X-ray wavelength region (XFEL) has been considered as a possible extension of the 3-GeV ERL light source proposed at KEK. In order to deliver a 6-GeV electron beam to the XFEL, the ERL is operated at the energy-doubling mode with a low average current. In this paper, we present results of electron beam simulations and FEL simulations for the XFEL proposed at KEK.

INTRODUCTION

Energy-recovery linac (ERL) to produce an electron beam of small emittance and high-average current is a promising technology for future light sources such as synchrotron radiation facility for coherent X-rays and laser Compton scattered γ -ray sources [1]. A collaborative project for the next-generation light sources based on energy-recovery linac has been established in Japan [2]. Critical components such as photocathode DC gun [3] and superconducting cavities [4] have been developed in JAEA and KEK. A test facility, the Compact ERL, is under construction to demonstrate the generation and acceleration of “ERL quality” electron beams. The first beam at the Compact ERL is scheduled in March 2013 [2].

One of the future ERL light sources under proposal in Japan is a synchrotron X-ray light source based on a 3-GeV ERL to be a successor of Photon Factory at KEK [5]. The 3-GeV ERL will offer far higher performance than the existing storage ring. The high repetition rate, short pulse, high spatial coherence and high brightness of ERL will drive forward a distinct paradigm shift in X-ray science from “static and homogenous” systems to “dynamic and heterogeneous” systems, in other words,

from “time- and space-averaged” analysis to “time- and space-resolved” analysis.

In addition, an X-ray FEL oscillator (XFEL) is proposed as a part of the ERL facility. The XFEL is driven by 6-GeV beam obtained from double-pass acceleration by main linac of the ERL as shown in Fig.1. The XFEL is operated at low repetition with small average current, thus, the energy recovery is not necessary. The XFEL to produce X-rays with full transverse and temporal coherence will be complementary to the undulator X-rays at the ERL [6].

In this paper, we describe design parameters of XFEL at the KEK ERL, results of electron beam degradation evaluation and XFEL simulations.

XFEL PARAMETERS AND GAIN

Bragg mirrors such as perfect crystals of diamond are used for the XFEL. Recently, Bragg mirrors having reflectivity more than 99% are becoming available at hard X-ray wavelengths [7]. We have, therefore, chosen FEL parameters to obtain small signal FEL gain larger than 30% to compensate the mirror loss and the extraction from the oscillator. Table 1 shows the parameters of electron beam, undulator and FEL gain for the XFEL, where the FEL wavelength is fixed at 1 Å as a representative example. Two sets of parameters are case (A) for typical electron beam parameters to obtain high-brilliant undulator radiation at the ERL, case (B) for shorter electron bunches with velocity bunching at the ERL main linac [8]. The case (B) with a smaller bunch charge is preferable for reducing thermal heat load on the Bragg mirrors. We plan to carry out beam dynamics studies specific to the XFEL such as small charge operation, velocity bunching in the Compact ERL.

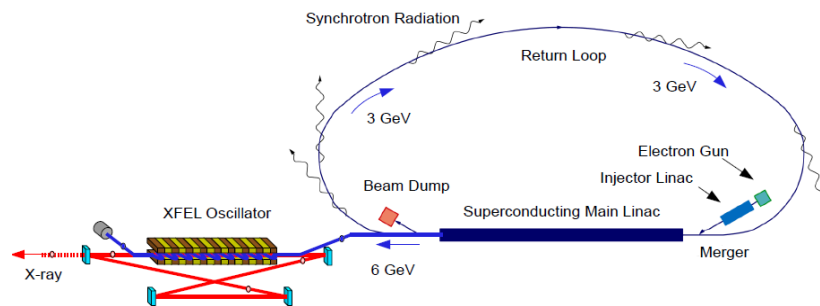


Figure 1: Conceptual layout of the 3-GeV ERL integrated with XFEL at KEK.

[#] hajima.ryoichi@jaea.go.jp

Table 1: Example Sets of XFELO Parameters

	Case (A)	Case (B)
E-beam		
Energy	6 GeV	→
Charge	20 pC	7.7 pC
σ_t	1 ps	0.38 ps
σ_E/E	5E-5	1.5E-5
ε_n	0.2 mm-mrad	→
β^*	17 m	→
Repetition	1 MHz	→
Undulator		
Pitch	1.94 cm	→
a_w	0.65	→
N_u	3000	→
FEL		
wavelength	1 Å	→
Gain	35%	63%

In an FEL oscillator, profile of the optical beam is determined by mirror geometry and the FEL gain depends on the filling factor, spatial overlap of the optical beam and the electron beam. The criterion of electron beam emittance to keep a good overlap with the optical beam is given by $\varepsilon_n/\gamma \leq \lambda/4\pi$, which is the diffraction limited electron beam. In the 6-GeV XFEL for 1 Å X-ray generation, the diffraction limited condition becomes $\varepsilon_n \leq 0.09\text{mm-mrad}$. We plot the small signal FEL gain as a function of normalized emittance in Fig. 2. The small signal gain for the diffraction limited condition is reduced to be 1/4 of the gain at zero emittance. Our design value of emittance is beyond the diffraction limit but we still have FEL gain large enough to compensate the total loss of X-ray resonator.

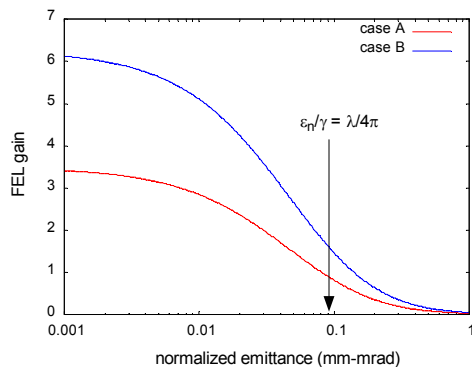


Figure 2: FEL small signal gain as a function of normalized emittance. The design value is 0.2 mm-mrad.

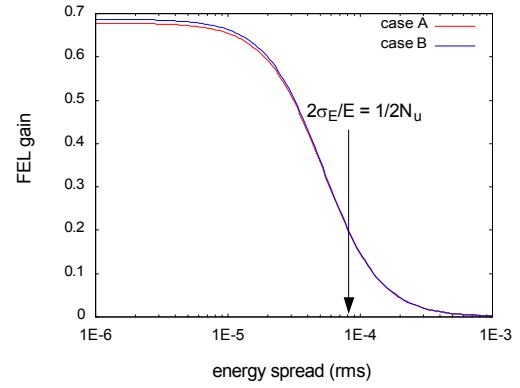


Figure 3: FEL small signal gain as a function of energy spread. The design value is 5E-5 for the case (A) and 1.5E-5 for the case (B).

Figure 3 shows the FEL small signal gain as a function of electron beam energy spread, σ_E/E . The indicator for the FEL gain bandwidth, $2\sigma_E/E \leq 1/2N_u$, is shown in the plot.

Figures 2 and 3 show that the FEL small signal gain is large enough for the XFEL lasing at 1 Å, if we achieve electron beam parameters listed in Table 1.

BEAM DEGRADATION IN THE ERL

In order to confirm the electron beam parameters after the double-pass acceleration at 3-GeV linac, we evaluated growth of emittance and energy spread by analytical and numerical manners.

In the analytical evaluation, we included incoherent radiation from bending magnets (ISR-bending) and undulators (ISR-undulator) as sources of beam degradation. Incoherent radiation from bending magnets introduces energy spread and emittance growth [9]:

$$\sigma_E^2 = \frac{55}{48\sqrt{3}} \frac{\hbar c e^2 \gamma^7}{\varepsilon_0 \rho^2}$$

$$\varepsilon_x = \frac{55}{96\sqrt{3}} \frac{\hbar c e^2 \gamma^7}{\varepsilon_0 \rho^2} \langle H_x \rangle$$

Assuming electron energy of 3 GeV, bending radius of 19.1 m and $\langle H_x \rangle = 3$ mm, we obtain

$$\frac{\sigma_E}{E} = 1.3 \times 10^{-5}$$

$$\varepsilon_x = 2.6 \times 10^{-13} \text{ m}$$

Incoherent radiation from undulators introduces energy spread and emittance growth [10]:

$$\sigma_E^2 = \frac{7}{15} \frac{e^2}{4\pi\varepsilon_0} \frac{\hbar}{mc} \left(\frac{2\pi}{\lambda_u} \right)^3 \gamma^4 K^2 F(K) L_u$$

$$\varepsilon_x \approx \frac{1}{2} \frac{\sigma_E^2}{E^2} \langle H_x \rangle$$

Assuming a 3-GeV ERL loop to accommodate undulators, 30 m x 6, 5 m x 22, and all the undulators are identical: $\lambda_u = 1.8$ cm, $K = 2$ and $\langle H_x \rangle = 0.082$ mm, we find the contribution of undulator incoherent radiation as

$$\frac{\sigma_E}{E} = 4.7 \times 10^{-5}$$

$$\varepsilon_x = 9.2 \times 10^{-14} \text{ m}$$

From the analytical evaluation, the effects of ISR-bending are found to be negligible and the emittance growth of ISR-undulator is also negligible. Energy spread induced by undulator radiation may affect the XFEL performance, if all the undulators in the ERL loop are closed to the minimum gap, $K=2$.

Next, we see the results of particle tracking simulations by elegant [11], where we conducted simulations from the merger (10 MeV) to the end of the second-pass acceleration (6 GeV) for the case (A) parameters in Table 1. The initial beam parameters at the merger are bunch charge 20 pC, rms bunch length 1 ps, normalized rms emittance 0.1 mm-mrad, rms energy

spread 0.2%. Incoherent and coherent radiation in bending magnets and short-range wakefield in superconducting cavities are taken into account, and no undulators are included in the simulations. The wakefield is based on a model of TESLA cavity [12], but the model seems similar to the ERL cavity. Detail description of the ERL loop is presented elsewhere [13].

Figure 4 shows evolution of transverse phase space from the merger to the end of the second-pass acceleration. We can see that the transverse emittance is almost preserved in spite of the small initial emittance.

Figure 5 is a plot of longitudinal phase space evolution. Growth of energy spread is not an issue either. The slight reduction of energy spread is attributed to the effects of CSR and cavity wakes.

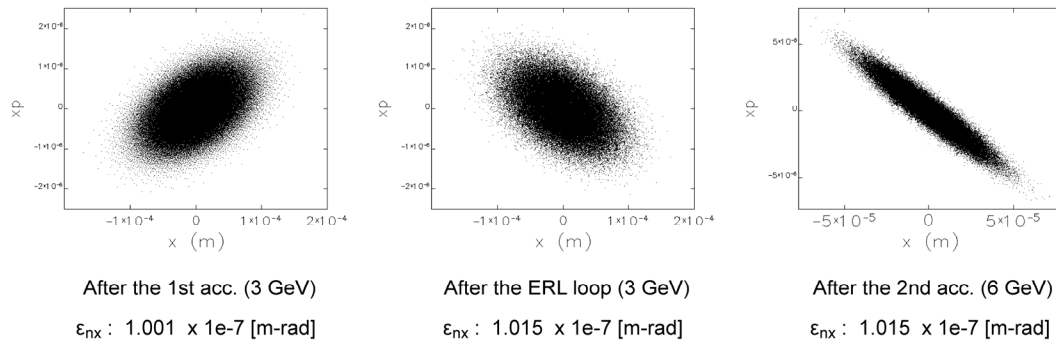


Figure 4: Evolution of transverse phase space of electrons obtained by particle tracking with Case (A) parameters.

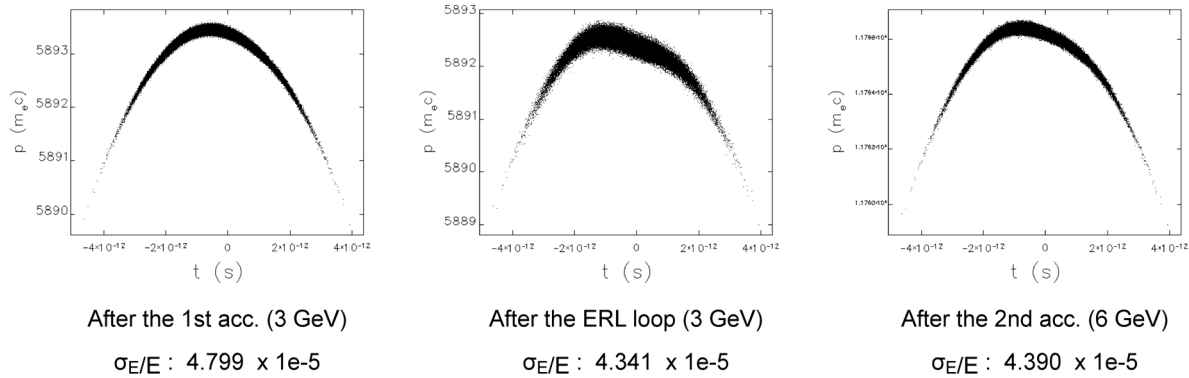


Figure 5: Evolution of longitudinal phase space of electrons obtained by particle tracking with Case (A) parameters.

XFEL SIMULATIONS

Performance of the proposed XFEL was studied by one-dimensional time-dependent FEL simulation code. A 3-D FEL simulation is inevitable to study high-gain SASE FELs, because transverse profile of the optical field is affected by electron beam, which is optical guiding or gain focusing. In FEL oscillators operated in the low-gain regime, the transverse profile of the optical field is determined by cavity geometry, and 1-D simulations give a good approximation. The simulation code used here was originally developed for an infrared FEL oscillator, which has been benchmarked by a series of experiments at the

JAERI-FEL: single super-mode, limit cycle, chaotic spiking and few-cycle pulse generation [14].

In the FEL simulations, Bragg mirrors in an XFEL are implemented as frequency filtering of an X-ray pulse every round trip. The temporal profile of an X-ray pulse at the undulator exit is converted into the frequency domain by fast Fourier transformation (FFT), and a frequency filter corresponding to the Bragg mirrors is applied. The filtered pulse is then converted back to the time domain by FFT. We use a model of Bragg mirrors, where reflectivity and phase shift are determined from the Darwin curve including absorption depending on X-ray energy [15].

Evolution of FEL power with parameters listed in Table 1, case (A), is plotted in Fig. 6. We assumed a triangular shaped electron bunch (rms 1 ps), Bragg mirrors having bandwidth of 10 meV and loss of 10% within the bandwidth. The simulation result shows that the FEL saturation occurs after 200 round trips.

Figure 7 shows evolution of FEL pulses for the same parameters. An FEL pulse starting with shot noise having no temporal coherence evolves gradually and has a smooth Gaussian-like profile after the saturation. The simulation result clearly shows the establishment of temporal coherence in the XFEL. The FEL pulse after the saturation has a temporal duration, 2.0 ps (FWHM), and the number of photons extracted from the oscillator is 2×10^9 /pulse for extraction efficiency of 5%.

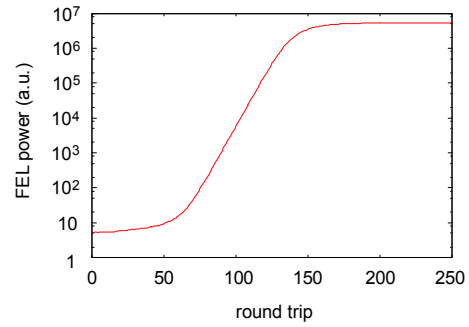


Figure 6: A result of FEL start-up simulation with the Case (A) parameters.

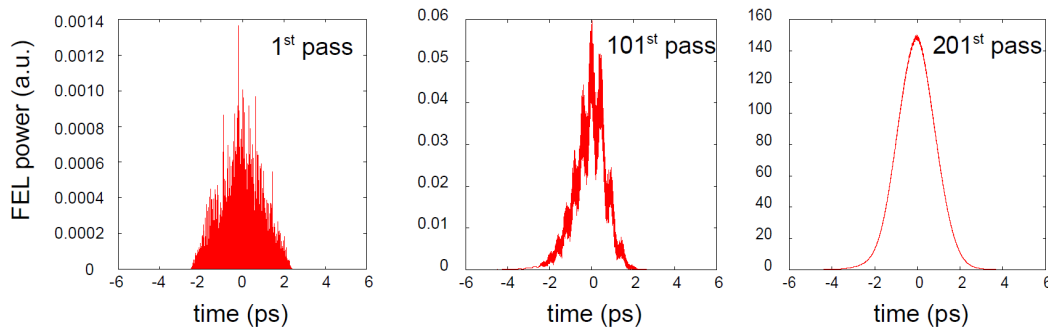


Figure 7: Evolution of a FEL pulse from shot noise to saturation.

SUMMARY

We have studied the performance of XFEL driven by a 6-GeV electron beam obtained from double-pass acceleration in the 3-GeV ERL planned at KEK. Assuming electron beam parameters similar to the normal 3GeV-ERL operation, we can obtain FEL gain large enough to operate the XFEL in the hard X-ray wavelength region.

Possible degradation of the electron beam during the ERL loop and linac has been studied both in analytical and numerical manners, where short-range wakefield in superconducting cavities, coherent and incoherent radiation from bending magnets and undulators are taken into account. As a result, we found that the emittance and energy spread are well preserved even after the double-pass acceleration.

We also conducted FEL simulations using a one-dimensional time-dependent code including a model of narrow-band Bragg mirrors. Evolution of FEL pulses from the shot noise to the saturation was calculated to show an FEL pulse with significant temporal coherence after the saturation.

Generation of an electron beam of “ERL quality” will be soon demonstrated in the Compact ERL, a test facility for future ERL light sources.

REFERENCES

- [1] R. Hajima, Rev. Acc. Sci. and Tech. 3 (2010) 121-146.
- [2] S. Sakanaka et al., Proc. IPAC-12, MOPPP018 (2012).
- [3] N. Nishimori, in these Proceedings.
- [4] K. Umemori et al., Proc. IPAC-12, MOOBC02 (2012); E. Kako et al., Proc. IPAC-12, WEPPC015 (2012).
- [5] Energy Recovery Linac Preliminary Design Report, IMSS/KEK (2012).
- [6] K-J. Kim et al., Phys. Rev. Lett. 100 (2008) 244802.
- [7] Y. Shvyd'ko et al., Nature Photonics 5 (2011) 1-4.
- [8] R. Hajima et al., Nucl. Instr. Meth. A637 (2011) S37-S42.
- [9] H. Wiedemann, “Synchrotron Radiation”, Springer (2003).
- [10] E.L. Saldin et al., Nucl. Instr. Meth. A381 (1996) 545-547.
- [11] M. Borland, Argonne. National Laboratory Advanced Photon Source Report No. LS-287 (2000).
- [12] TESLA Technical Design Report (2001).
- [13] M. Shimada et al., Proc. Particle Acc. Soc. Jpn. (2012) (in Japanese).
- [14] R. Nagai et al., Nucl. Instr. Meth. A483 (2002) 129-133.
- [15] R. Hajima et al., Proc. FEL-2008 (2008) 87-89.